12TH CANADIAN CONFERENCE ON EARTHQUAKE ENGINEERING
JUNE 17-20, 2019
CHÂTEAU FRONTENAC
QUÉBEC, QC.
12ÈME CONFÉRENCE CANADIENNE DU GÉNIE PARASISMIQUE
17-20 JUIN 2019
CCEE 2019

Methodology for the reassessment of magnitudes assigned to historical earthquakes

Alessandro Stocchi[1], Cédric Giry[2], Irmela Zentner[3], Emmanuelle Nayman[4], Sophie Capdevielle[5], Frédéric Ragueneau[6]

[1] PhD, LMT, ENS Cachan, CNRS, Université Paris-Saclay, 94235 Cachan, France.
[2] Ast. Prof., LMT, ENS Cachan, CNRS, Université Paris-Saclay, 94235 Cachan, France.
[3] PhD, Eng., EDF R&D Lab Paris-Saclay. 91120 Palaiseau, France.
[4] Eng., EDF – DIPNN Direction Industrielle – TEGG, 13097 Aix-en-Provence, France.
[5] PhD, LMT, ENS Cachan, CNRS, Université Paris-Saclay, 94235 Cachan, France.
[6] Prof., LMT, ENS Cachan, CNRS, Université Paris-Saclay, 94235 Cachan, France.

ABSTRACT

This work proposes a framework for the reevaluation of the intensity based on probabilistic method and structural analysis. The method developed in this work allows for an update of the magnitude of historical earthquakes based on structural fragility functions and comparison to the damage observed in situ. It builds on an approach initially proposed by Ryu and Baker, who applied Bayesian updating to re-evaluate magnitudes of earthquakes based on the distribution of the damage states of the building stock. The goal of this work is to assess the feasibility of the approach initially proposed by Ryu et al. to the distinct fragile structures. The Bayesian updating procedure allows for accounting for uncertainty related to the structural response, ground motion and site parameters. It also introduces a priori information from seismic catalogue in a straightforward manner.

Several structures in the area considered, still existing nowadays, have been submitted to the historical earthquakes. Among them, a large number of masonry structures such as simple houses, small castles, industrial buildings are considered for this study.

Keywords: Historical earthquakes; vulnerability analysis; masonry; Bayesian approach.

INTRODUCTION

At the end of the nineteenth century, France has encountered several large earthquakes. However, given the small amount of data and testimonies collected that can be used to quantify these historical earthquakes, uncertainties related to the macro-seismic intensity but also to the epicenter location associated to these events are considered as rather high. For example, we consider a site where no considerable damage has been reported in historical documents found up to now. In consequence, the epicentral intensity and epicenter location assigned to these events in the earthquake catalogue are labeled respectively as "peu sûr" and very uncertain. This means that Epicentral intensity might be overestimated and epicenter location might be elsewhere.

For about 40 years, having been started in support of the development of the nuclear industry in France, efforts have been jointly made by BRGM (Bureau de Recherche Géologique et Minière), EDF (Electricité de France) and IRSN (Institut de Radioprotection et Sûreté Nucléaire) to collect, compile, and distribute information related to historical events. The SISFRANCE macroseismic database contains 100,000 macroseismic observations (MSK intensity scale [1]) associated to 6000 earthquakes (AD463-2007). These Intensity Data Points (IDPs) are representative of earthquake effects in terms of damages and population perception at various localities. The descriptions of these effects, used to assess intensity values are collected from historical archives for each event. Epicentral location is determined and provided, together with the epicentral intensity value when possible (see [2] for epicentral location and intensity assessment explanations). IDPs are associated to quality factors that reflect confidence related to numerical value (quality A: certain intensity, quality B: fairly certain intensity, quality C: uncertain intensity). Epicentral intensity estimates are also associated to quality factors (quality A: certain epicentral intensity; quality B: fairly certain epicentral intensity; quality C: uncertain epicentral intensity, quality E: arbitrary epicentral intensity; quality K: fairly certain epicentral intensity, resulting from a calculation based on intensity attenuation).

According to the occurrence date of earthquakes and/or their location with respect to France borders, macroseismic field configuration can be observed in the SISFRANCE database as follows: (i) recent and largest events, located inside or close to the borders, exhibiting large and well distributed macroseismic field, (ii) off-shore or cross border events, characterized by a lack of information at short distances but with reliable data at greater distances, and (iii) old events associated with a poorly constrained macroseismic field, where either the epicentral intensity is only quantitatively known or no intensity value is available, expect for few felt testimonies.A reecent methodology [3] proposes to introduce structural analyses in the process of definition of the macroseismic intensity of historical earthquakes. The main idea is to update the distribution of intensities or magnitudes of the considered earthquake by means of a Bayesian approach, combining the use of input data fragility curves and in-situ observed damages.

In the context of the French metropolitan territory, characterized by low to moderate seismic activity, and a large amount of old structures as well as cultural heritage, this methodology appears to be an interesting way to reanalyze historical earthquakes. The work exposed in this paper applies the methodology proposed in [3] to a historical earthquake in France.

In a first part of this work, numerical tools have been developed to generate parametric numerical models for the description of the different typologies of building observed in the area of interest. In a second part, the nonlinear response of the buildings is computed according to pushover analysis in order to identify the parameters of an equivalent nonlinear simple oscillator. Unless its simplicity and the use of strong hypothesis, the nonlinear simple oscillator allows for global responses and for obtaining information regarding the damage state of the structure considering global indicators. In a third step, these simple nonlinear models are used to compute fragility curves for the different typologies of structures . In this part, the definition of criteria to define the damage of the structure is also discussed.

PARAMETRIC MODEL OF MASONRY BUILDING

Description of the masonry typology of interest

The industrial development in the nineteenth century have seen the construction of a large number of masonry buildings in France. This type of building is characterized by a regular shape with a homogeneous distribution of the openings and a regular height of the story (Figure 1).

Figure 1: Sample of an old industrial building in masonry

These simple characteristics allow to develop a parametric model with a relatively small number of parameters in order to cover a large panel of buildings in this typology. In addition, in the context of seismic vulnerability analysis, this type of building falls within the range of time period with the highest spectral acceleration in the area of interest. Indeed, according to the simple formula for the estimation of the fundamental period T_1 of the structure given by Eq. $T_1 = C_t H^{\frac{3}{4}}$ *(1)* [4], the range of period for these buildings is around 0.28 - 0.38 s (height of the building between 10 m and 15 m). The plateau of the regulatory spectral acceleration goes from 0.06 s up to 0.4 s.

$$T_1 = C_t H^{\frac{3}{4}} \qquad (1)$$

C_t is the coefficient accounting fort he type of buildings (0.05 for masonry building) and H ist he total height of the building.

Automatic mesh generator

The French metropolitan territory is characterized by low to moderate seismic activity. Therefore, the observed damage (e.g. cracking) tends not to appear or to be small for this type of building. In order to model this type of behavior, a continuous modeling with a homogeneous description of the masonry seems to be relevant. In order to reduce the number of degrees of freedom (dof) of the model, the slabs and walls are described with shell element.

Each building is defined by the size of a story (length, width and height), the number of stories, the location and size of the opening. The generation of the geometry and the mesh, according to these characteristics, is obtained with a set of Python files developed for this study and libraries of SALOME [5].

Figure 2 show two examples of mesh generated with the tools developed for two different typologies of building (house and industrial building).

a)

b)

Figure 2: Example of mesh generated for different typologies of old masonry building. a) house; b) industrial building

VULNERABILITY ANALYSIS OF THE BUILDING

Simplified modeling of the structural response

In the context of fragility analysis combined with a parametric variability of the properties of the building, a large number of computations is needed. In order to tackle this problem, a simplified modeling of the nonlinear response of the structure is developed.

The displacement field $\boldsymbol{U}(t)$ can be expressed on the modal basis according to Eq. $\boldsymbol{U}(t) = \sum_i q_i(t)\,\boldsymbol{\phi}_i = \boldsymbol{P}\boldsymbol{q}(t)$ *(2)*:

$$\boldsymbol{U}(t) = \sum_i q_i(t)\,\boldsymbol{\phi}_i = \boldsymbol{P}\boldsymbol{q}(t) \qquad (2)$$

$\boldsymbol{\phi}_i$ and $q_i(t)$ are the eigenvector and the modal displacement of the mode i. $\boldsymbol{P}$ is the matrix of the modal basis. A mass normalization ($\boldsymbol{\phi}_i^T \boldsymbol{M} \boldsymbol{\phi}_i = 1$) is adopted for the development of the equation of motion in the modal basis.

In the context of low to moderate damage for regular buildings, it is assumed that the mode shape is not modified. Furthermore, the energies stored or dissipated in the system are considered to evolve independently for each mode. This framework is similar to those proposed for modal pushover analysis [6,7]. The free energy ψ in the structure is decomposed on each mode Eq. $\psi(\boldsymbol{U}, \ldots) = \sum_i \psi_i(q_i, V_i)$ *(3)*.

$$\psi(\boldsymbol{U}, \ldots) = \sum_i \psi_i(q_i, V_i) \qquad (3)$$

V_i are the internal variables associated to the model of mode i (damage, plasticity…). The dissipation $\mathcal{D}_{vis}$ associated to viscous damping also decomposed on each mode shape Eq. $\mathcal{D}_{vis}\left(\dot{\boldsymbol{U}}, \ldots\right) = \sum_i \mathcal{D}_{vis_i}(\dot{q}_i) = \sum_i \frac{1}{2} c_i \dot{q}_i^{\,2} = \sum_i \frac{1}{2} 2\xi_i \omega_i \dot{q}_i^{\,2}$ *(4)*.

$$\mathcal{D}_{vis}\left(\dot{\boldsymbol{U}}, \ldots\right) = \sum_i \mathcal{D}_{vis_i}(\dot{q}_i) = \sum_i \frac{1}{2} c_i \dot{q}_i^{\,2} = \sum_i \frac{1}{2} 2\xi_i \omega_i \dot{q}_i^{\,2} \qquad (4)$$

As the mass matrix $\boldsymbol{M}$ does not evolve, the kinetic energy $\mathcal{T}$ can be decomposed independently on each mode Eq. $\mathcal{T}\boldsymbol{U}, \ldots$ ⍰ $= \sum_i \mathcal{T}_i(\dot{q}_i) = \sum_i \frac{1}{2} \boldsymbol{\phi}_i^T \boldsymbol{M} \boldsymbol{\phi}_i \dot{q}_i^{\,2} = \sum_i \frac{1}{2} m_i \dot{q}_i^{\,2}$ *(5)*.

$$\mathcal{T}\left(\dot{\boldsymbol{U}}, \ldots\right) = \sum_i \mathcal{T}_i(\dot{q}_i) = \sum_i \frac{1}{2} \boldsymbol{\phi}_i^T \boldsymbol{M} \boldsymbol{\phi}_i \dot{q}_i^{\,2} = \sum_i \frac{1}{2} m_i \dot{q}_i^{\,2} \qquad (5)$$

Furthermore, the mathematical expression of the generalized force Q_i associated to the seismic loading on mode i, does not evolve Eq. $Q_i = -\sum_k \boldsymbol{\phi}_i^T \boldsymbol{M} \boldsymbol{\Delta}_{\boldsymbol{k}} a_{g_k}(t)$ *(6)*.

$$Q_i = -\sum_k \boldsymbol{\phi}_i^T \boldsymbol{M}\boldsymbol{\Delta}_{\boldsymbol{k}} a_{g_k}(t) \qquad (6)$$

$a_{g_k}(t)$ is the accelerogram in the direction k, $\boldsymbol{\Delta}_{\boldsymbol{k}}$ is the vector associated to the direction k.

By using the Lagrange equations Eq. $\frac{d}{dt}\left(\frac{\partial \mathcal{L}}{\partial \dot{q}_i}\right) - \left(\frac{\partial \mathcal{L}}{\partial q_i}\right) = Q_i - \left(\frac{\partial \mathcal{D}_{vis}}{\partial \dot{q}_i}\right)$ *(7)*, one can get the equation of equilibrium on each mode Eq. $\ddot{q}_i(t) + 2\xi_i\omega_i\dot{q}_i(t) + f_{int}^i[q_i(t)] = -\sum_k \boldsymbol{\phi}_i^T \boldsymbol{M}\boldsymbol{\Delta}_{\boldsymbol{k}} a_{g_k}(t)$ *(8)*.

$$\frac{d}{dt}\left(\frac{\partial \mathcal{L}}{\partial \dot{q}_i}\right) - \left(\frac{\partial \mathcal{L}}{\partial q_i}\right) = Q_i - \left(\frac{\partial \mathcal{D}_{vis}}{\partial \dot{q}_i}\right) \qquad (7)$$

$\mathcal{L}$ is the Lagrangian of the structure and is equal to: $\mathcal{L} = \mathcal{T} - \psi$.

$$\ddot{q}_i(t) + 2\xi_i\omega_i\dot{q}_i(t) + f_{int}^i[q_i(t)] = -\sum_k \boldsymbol{\phi}_i^T \boldsymbol{M}\boldsymbol{\Delta}_{\boldsymbol{k}} a_{g_k}(t) \qquad (8)$$

$f_{int}^i[q_i(t)]$ is the internal force associated to mode i. Its expression derived from the free energy ψ_i Eq. $f_{int}^i[q_i(t)] = \frac{\partial \psi}{\partial q_i} = \frac{\partial \psi_i}{\partial q_i}$ *(9)*.

$$f_{int}^i[q_i(t)] = \frac{\partial \psi}{\partial q_i} = \frac{\partial \psi_i}{\partial q_i} \qquad (9)$$

The model used for the modal response can be more or less complex according to the nonlinear phenomena considered. It is identified thanks to the global response of the structure submitted to a displacement field proportional to the mode shape analyzed: $\boldsymbol{\delta}_{load} = \lambda\boldsymbol{\phi}_i$. The coefficient λ can be directly identified as the modal displacement q_i. For the internal force, a conversion factor is used to identify f_{int}^i. By considering the direction k as the main direction of the mode considered, one can identified f_{int}^i with the base shear force V_{b_k} and the modal participation factor $p_{i_k}$of mode i in the direction k. Eq. $V_{b_k} = \boldsymbol{\Delta}_k^{\mathrm{T}}(\lambda \boldsymbol{K}\boldsymbol{\phi}_i) = \lambda \sum_i p_{i_k} \boldsymbol{\phi}_i^T \boldsymbol{K}\boldsymbol{\phi}_i = p_{i_k}\omega_i^2\lambda \rightarrow f_{int}^i(q_i) = \omega_i^2 q_i = \frac{V_{b_k}}{p_{i_k}}$ *(10)* provides this coefficient with the example of linear behavior for the mode i.

$$V_{b_k} = \boldsymbol{\Delta}_k^{\mathrm{T}}(\lambda \boldsymbol{K}\boldsymbol{\phi}_i) = \lambda \sum_i p_{i_k} \boldsymbol{\phi}_i^T \boldsymbol{K}\boldsymbol{\phi}_i = p_{i_k}\omega_i^2\lambda \rightarrow f_{int}^i(q_i) = \omega_i^2 q_i = \frac{V_{b_k}}{p_{i_k}} \qquad (10)$$

This conversion is consistent with the one that can be done for pushover analysis (i.e. definition of the capacity in the acceleration displacement unit system: $V^*(d^*)$). Indeed, for the general case without the mass normalization, one can get Eq. $\frac{\omega_i^2}{m_i} q_i = \frac{V_{b_k}}{p_{i_k}} \rightarrow \omega_i^2 \frac{q_i}{p_{i_k}} = \frac{V_{b_k}}{p_{i_k}^2} m_i \rightarrow \omega_i^2\, d^* = \frac{V_{b_k}}{m_i^{eff}} = V^*$ *(11)* for the relation between q_i and V_{b_k}.

$$\frac{\omega_i^2}{m_i} q_i = \frac{V_{b_k}}{p_{i_k}} \rightarrow \omega_i^2 \frac{q_i}{p_{i_k}} = \frac{V_{b_k}}{p_{i_k}^2} m_i \rightarrow \omega_i^2\, d^* = \frac{V_{b_k}}{m_i^{eff}} = V^* \qquad (11)$$

In order to get the curve $V^*(d^*)$, the conversion factor for the displacement is so the participation factor for mode i in direction k and for the force the effective modal mass for mode i in direction k.

From the nonlinear analysis on the full structure, one can identify the parameter of the single degree of freedom (SDOF) model for the mode thanks to a minimization of the error between the response of the model and the response obtained with the 3D finite element model (V_{b_k}, λ). In order to limit the number of 3D nonlinear analysis, only the first main modes are considered for nonlinear behaviour. The higher modes are considered to remain linear with properties obtained directly from the modal analysis.

Figure 3 illustrates the global process for the identification of the SDOF model of the modes.

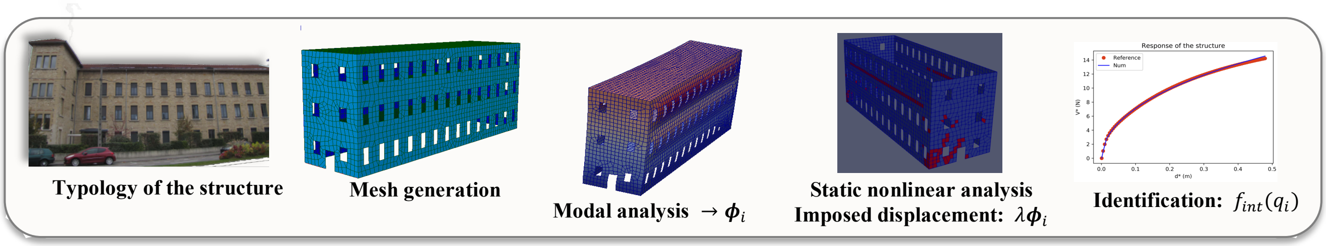

Figure 3: Procedure for the identification of the SDOF nonlinear model of the modes

The response of the structure submitted to a seismic loading is then computed on the modal basis. This simplified modelling allows, by modal recombination, to get the displacement of each point of the structures. Furthermore, according to the nonlinear SDOF model used, one can get global damage indicator like the frequency shift for nonlinear mode. This information is used to define criteria of failure for fragility curves.

The nonlinear model used to characterize the behavior of the masonry is an isotropic damage model proposed initially for concrete [8]. The computations of the 3D FE model have been performed with Code_Aster [9].

For the nonlinear SDOF behavior of a mode a unilateral damage model is considered. Eq. $\psi_i(q_i, D_i^+, D_i^-) = \frac{1}{2}k_i(1-D_i^+) < q_i >_+^2 + \frac{1}{2}k_i(1-D_i^-) < q_i >_-^2$ *(12)* gives the free energy of this model.

$$\psi_i(q_i, D_i^+, D_i^-) = \frac{1}{2}k_i(1-D_i^+) < q_i >_+^2 + \frac{1}{2}k_i(1-D_i^-) < q_i >_-^2 \qquad (12)$$

k_i is the initial modal stiffness, D_i^+ and D_i^- are respectively the damage associated to the positive modal displacement and to the negative modal displacement. The internal force is obtained by deriving the free energy according to the modal displacement Eq. $f_{int}^i[q_i(t)] = \frac{\partial \psi_i}{\partial q_i} = k_i(1-D_i^+) < q_i >_+ + k_i(1-D_i^-) < q_i >_-$ *(13)*:

$$f_{int}^i[q_i(t)] = \frac{\partial \psi_i}{\partial q_i} = k_i(1-D_i^+) < q_i >_+ + k_i(1-D_i^-) < q_i >_- \qquad (13)$$

A threshold function is defined for each damage variable as a function of the elastic energy release rate ($Y_+ = \frac{1}{2}k_i < q_i >_+^2$ and $Y_- = \frac{1}{2}k_i < q_i >_-^2$) Eq. $f_+ = Y_+ - Y_0\left(\frac{d_\infty}{d_\infty - D_i^+}\right)^{\frac{1}{b}} \leq 0 \;\;|\;\; f_- = Y_- - Y_0\left(\frac{d_\infty}{d_\infty - D_i^-}\right)^{\frac{1}{b}} \leq 0$ *(14)*

$$f_+ = Y_+ - Y_0\left(\frac{d_\infty}{d_\infty - D_i^+}\right)^{\frac{1}{b}} \leq 0 \;\;|\;\; f_- = Y_- - Y_0\left(\frac{d_\infty}{d_\infty - D_i^-}\right)^{\frac{1}{b}} \leq 0 \qquad (14)$$

d_∞ and b are parameters defining the evolution of the threshold function. Y_0 corresponds to the limit energy of the linear behavior. Damage evolve by respecting the Kuhn-Tucker conditions. By considering the condition $f_i = 0$ when damage evolves, one can get the damage evolution law Eq. $D_i^+ = d_\infty\left[1 - \left(\frac{Y_0}{Y_+}\right)^b\right] \;\;|\;\; D_i^- = d_\infty\left[1 - \left(\frac{Y_0}{Y_-}\right)^b\right]$ *(15).*

$$D_i^+ = d_\infty\left[1 - \left(\frac{Y_0}{Y_+}\right)^b\right] \;\;|\;\; D_i^- = d_\infty\left[1 - \left(\frac{Y_0}{Y_-}\right)^b\right] \qquad (15)$$

This model allows to compute easily criteria of frequency shift without using the recombination to get the global behavior of the structure. The damage frequency f_D^i of the mode i and the damage level D corresponding to a frequency shift Δf are obtained with Eq. $f_D^i = \sqrt{1-D}f_0^i \;|\; \Delta f = \frac{f_0^i - f_D^i}{f_0^i} \rightarrow D = 1 - \Delta f^2$ *(16).*

$$f_D^i = \sqrt{1-D}f_0^i \;|\; \Delta f = \frac{f_0^i - f_D^i}{f_0^i} \rightarrow D = 1 - \Delta f^2 \qquad (16)$$

D is the maximum damage level reach by the mode i ($D = \max[D_i^+, D_i^-]$) and f_0^i is the initial frequency of the mode i.

Computation of fragility curves

Fragility curves express the conditional probability of failure P_f of the structure for a given seismic Intensity Measure IM denoted α. In this study, the failure is defined by a criterion related to the frequency shift and the Intensity Measure is the peak ground acceleration – PGA. From the fragility curve, one can define a probability of non-failure, according to a damage level d for an intensity level α Eq. $P(d|\alpha) = 1 - P_f(\alpha)$ *(17).*

$$P(d|\alpha) = 1 - P_f(\alpha) \qquad (17)$$

To reduce the number of calculations of the structural response under seismic loadings, the classical lognormal fragility model is used [10]. The computation of the two parameters defining the fragility curve Eq. $Pf\alpha = \Phi\left(\frac{ln\left(\frac{\alpha}{Am}\right)}{\beta}\right)$ *(18)* is performed thanks to the maximum likehood methodology [11].

$$P_f(\alpha) = \Phi\left(\frac{ln\left(\frac{\alpha}{A_m}\right)}{\beta}\right) \quad (18)$$

A_m is the median capacity and β is the logarithmic standard deviation.

MAGNITUDE ESTIMATION OF HISTORICAL EARTHQUAKE

The analysis presented here to reevaluate the magnitude of an historical earthquake is based on the methodology proposed by [3]. In the present work, the approach is slightly modified so as to investigate the magnitude of "small" earthquakes. Indeed, the structures considered are the ones that have not encountered damage or only relatively small degradations. The main objective is to analyze if the magnitude in the earthquake catalogue is consistent with the state of the structures that have experienced the historical earthquake. The methodology proposed by [3] is briefly recalled and is then applied to the case studied.

Methodology

The estimation of a posteriori magnitude is obtained by Bayesian updating of the a priori magnitude distribution $f_M(m)$ of the considered earthquake. This requires the knowledge d if the structure is damaged or not. The a posteriori or updated distribution of the magnitude $f(m|d)$ is computed according to Eq. $f_{M|d}(m|d) = \frac{P(d|M=m)f_M(m)}{\int P(d|M = m)f_M(m)dm}$ (19) as:

$$f_{M|d}(m|d) = \frac{P(d|M=m)f_M(m)}{\int P(d|M = m)f_M(m)dm} \quad (19)$$

This actualization needs the probability $P(d|m)$ of damage observation d for a given magnitude m Eq. $P(d|m) = \iiint P(d|\alpha)f_{IM}(\alpha|m,r,s)f_R(r)f_S(s)dr\, ds\, d\alpha$ (20). The latter is also called likelihood function and is here expressed as

$$P(d|m) = \iiint P(d|\alpha)f_{IM}(\alpha|m,r,s)f_R(r)f_S(s)dr\, ds\, d\alpha \quad (20)$$

The functions $f_R(r)$ and $f_S(s)$ allow to introduce respectively the uncertainties relative to the localization of the earthquake and to the site proxies (e.g. resonant frequency, VS30).

The function $f_{IM}(\alpha|m,r,s)$ corresponds to a Ground Motion Prediction Equation (GMPE) using site proxies.

Characterization of historical earthquake

According to the earthquake catalogue FCAT-17 [12], the considered earthquake has an average moment magnitude of M_w = 4.4 with a standard deviation equal to 0.42. This information is used to define the a priori magnitude distribution. Different choices for the prior distribution are investigated:

- Gaussian distribution centered on the average M_w with the standard deviation given by the catalogue,
- Gaussian distribution centered on the average M_w with a higher standard deviation in order to include a possible error on the macro-seismic initial classification
- Uniform distribution

Currently, as no GMPE including site proxies for the specific studied region exists, the GMPE developed by [13] for Japanese data has been considered. This GMPE has been established with the Japannese KiK-net data. It has the advantage of depending on the fundamental frequency of the site, which is used as a site proxy in this work. The GMPE has been derived by means of Artificial Neural Network. The parameters defining the neural network are given in [13].

For this study, no uncertainty is considered for the site proxies. For the localization of the earthquake, an uncertainty regarding the depth is introduced through a lognormal distribution.

Fragility curve for masonry industrial building

The reassessment of the magnitude is illustrated with an example considering fragility analysis on a masonry industrial building corresponding to the typology illustrated on Figure 3. The global sizes of this building are: 14 m, 40 m, 6 m (width, length, height). The windows are regularly spaced. The nonlinear behavior of the masonry is modeled for the pushover analysis by considering Mazars model. Standard values are used for the elastic characteristics of the masonry.

Figure 4 illustrated the nonlinear response obtained with the pushover analysis for the first mode and the response of the SDOF model after the identification of its parameters by minimization process.

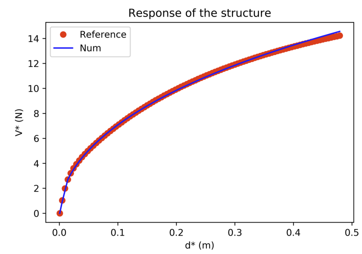

Figure 4: Response of the structure for the first mode (red points) and for the identified nonlinear SDOF model (blue line).

The building studied doesn't show any damage. Furthemore no damage is reported in the testimonies link to the historical earthquake studied. As a consequence, a criterion of light damage is considered to compute the fragility curve. Furthermore, the probability of non-failure is used in the next part of the study. The light damage criterion is expressed by a frequency shift of the nonlinear mode of 15%.

Figure 5 shows the fragility curve for the cases corresponding to the failure mode of a frequency shift of 15%, 30% and 50% for a standard industrial building. The parameter α considered here is the PGA.

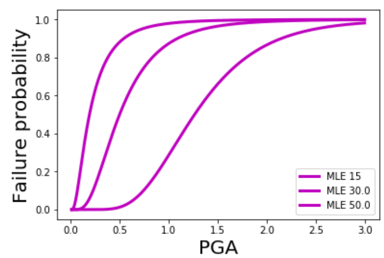

Figure 5: Fragility curve for failure mode of 15%, 30% and 50% frequency shift

Reassessment of the magnitude with masonry industrial building

Thanks to a Bayesian updating process the initial magnitude distribution using the information from the catalogue can be updated. A first example is shown by considering for the characterization of the structure the fragility curve corresponding to a light damage state (frequency shift of 15%) for the structures studied. Figure 6 shows the prior and the updated magnitude distributions according to this criteria.

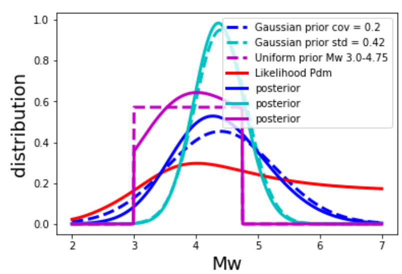

Figure 6: A priori and a posteriori magnitude considering fragility curve with a criteria of 15% frequency shift

In order to consider the fact that different damage states have been observed by the buildings, a multinomial distribution is used to compute $P(d|M = m)$.

$$P(d|\alpha) = \frac{n_{t_b}!}{\prod_{k=0}^{n_{d_b}} n_k!} \times \prod_{k=0}^{n_{d_b}} P(d_m = d_{m_k}|\alpha) \qquad (21)$$

d_m is the damage state, d_{m_k} a damage state criteria (e.g. no damage, light damage, …), n_{t_b} the total number of buildings observed and n_{d_b} the number of damage states in the set of buildings considered. As for the most part of the industrial masonry building no damage has been observed, the example given in is computed by considering five buildings in the area of interest (four buildings without damage and one building with light damage (15% frequency shift reach)).

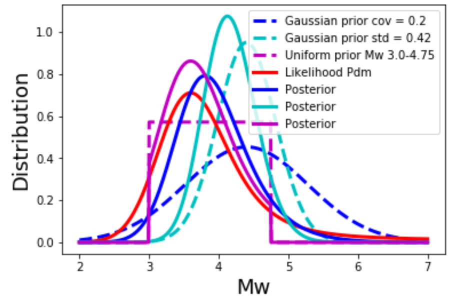

Figure 7: A priori and a posteriori magnitude a set of observation (four buildings without damage and one with light damage)

As illustrated on these simple analyses, the introduction of the supplementary knowledge in the magnitude assessment allows increasing the confidence in the expected value of the magnitude while its standard deviation decreases.

CONCLUSIONS

A methodology to reassess the magnitude of historical earthquakes has been applied in this work. The information relative to the studied historical earthquake has been extracted from a large French database. As the level of uncertainty is relatively high for some earthquakes, supplementary information on building damage states is introduced in order to update the prior knowledge on the magnitude distribution by means of a Bayesian approach. In order to integrate a large number of data coming from the observations made on old masonry buildings, an automatic mesh generator has been developed. In order to investigate the vulnerability of these buildings for a large number of seismic scenarios, a simplified modeling strategy is proposed. The 3D model is used to determine the parameters of the SDOF model associated to each mode and the nonlinear time history analysis for earthquake loading are then performed with the simplified model. These models are used in the process of magnitude estimation of historical earthquake to compute efficiently fragility curves. The Bayesian process and the global methodology for the magnitude estimation has been briefly recalled and illustrated with an analysis of industrial masonry building. This method tends to be promising to reassess historical earthquakes. This project is an ongoing work in which several typologies and variability in a same typology are investigated to cover a large panel of data available from in-situ observations.

REFERENCES

[1] Medvedev, S. V. and W. Sponheuer (1969). Scale of Seismic Intensity, *Proc. World Conf. Earthquake Eng., 4th, Santiago, Chile*, A2, 143-153.

[2] Lambert J, Montfort-Climent D, Bouc O (2015) Catalogue of isoseismal areas for XXth century french historical earthquakes (Io [VI). *BRGM report* BRGM/RC-66444-FR

[3] Ryu H, Kim J.K, Baker J.W (2009) A Probabilistic Method for the Magnitude Estimation of a Historical Damaging Earthquake Using Structural Fragility Functions. *Bulletin of the Seismological Society of America,* 99(2A):520-537.

[4] CEN. Design of structures for earthquake resistance, Part 1: General rules, seismic actions and rules for buildings. EN 1998-1. Brussels: CEN 2004, 232 p.

[5] CEA, EDF, OpenCascade. SALOME software: https://www.salome-platform.org/

[6] Chopra A. K., Goel R. K. A Modal Pushover Analysis Procedure to Estimate Seismic Demands for Buildings: Theory and Preliminary Evaluation. *PEER Report n° 2001/03*. Berkeley: University of California, 2001, 90 p.

[7] Tataie, L., Brun, M., Reynouard, J.-M. (2012). Modal pushover procedures for seismic evaluation of reinforced concrete structures: using new nonlinear single degree of freedom systems. *European Journal of environment and Civil Engineering*, 16(2) :178-203.

[8] Mazars, J. (1984). Application de la mécanique de l'endommagement au comportement non linéaire et à la rupture du béton de structure. Thèse d'état, Université Paris 6.

[9] EDF. Code_Aster software. https://www.code-aster.org/

[10] Reed, J.W., Kennedy, R.P., (1994). Methodology for Developing Seismic Fragilities. *Final Report TR-103959*, *EPRI.*

[11] Shinozuka, M., Feng, Q., Lee, J. and Naganuma, T. (2000). Statistical analysis of fragility curves. *J. Eng. Mech. ASCE*, 126(12):1224-1231.

[12] Manchuel, K., Traversa, P., Baumont, D., Cara, M., Nayman, E., Durouchoux, C. (2017). The French seismic CATalogue (FCAT-17). *Bull Earthq Eng.*, 16(6):2227-2251

[13] Derras, B., Bard, P-Y., Cotton, F., Bekkouche, A., (2012). Adapting the neural network approach to PGA prediction: an example based on the KiK-net data. *Bulletin of the Seismological Society of America* 102:1446–1461.